Environmental Dependence of the Galaxy Mass–Size Relation from HST and JWST Observations

Mahtab Armand*[1,2] and Moein Mosleh†[1,2]

[1]Biruni Observatory, School of Science, Shiraz University, Shiraz 71454, Iran
[2]Department of Physics, School of Science, Shiraz University, Shiraz 71454, Iran

Abstract

Understanding whether galaxy structural evolution is primarily driven by internal processes or influenced by the surrounding environment remains a key question in galaxy evolution. We investigate the environmental dependence of the mass-size relation and structural properties of star-forming and quiescent galaxies using complementary observations from HST and JWST over the redshift range ($0.5 < z < 3.0$). The first analysis is based on approximately 3,000 galaxies observed with HST, where structural parameters are measured from two-dimensional stellar mass maps, minimizing the effects of color gradients and spatial variations in the stellar mass-to-light ratio. We then extend the study using nearly 10,000 galaxies observed with JWST, deriving structural parameters from high-resolution F444W imaging to probe the same question with substantially improved depth, spatial resolution, and statistical power. Across both datasets, the galaxy mass–size relation shows little to no environmental dependence for either star-forming or quiescent galaxies. The consistency between the stellar mass-based measurements from HST and the light-based structural measurements from JWST shows that the lack of significant environmental trends holds across differences in sample size, observational wavelength, and measurement technique. These results suggest that, over the redshift range $0.5 < z < 3$, internal evolutionary processes predominantly govern galaxy structural evolution.

Keywords: *Galaxies: evolution — Galaxies: structure — Galaxies: high-redshift — Environmental effects — Cosmology: observations*

1. Introduction

Galaxies are not distributed randomly; they exist in cosmic filaments, walls, groups, clusters, and voids. Some processes may affect the structure of galaxies, such as gravitational processes (mergers, tidal interactions, harassment), gas-related processes (ram-pressure stripping, strangulation, gas compression), and environmental potential processes (tidal stripping, dynamical friction, cluster potential). However, the extent and nature of the impact of these processes on galaxy structure remain an open question.

This has been investigated in many studies, though most of them have been conducted at low redshift ($z < 0.5$) (Abdullah, 2026, Ding & et al., 2024). Only a few studies have explored the relationship between galaxies and their environment at high redshift ($z \geq 0.5$) (Allen & et al., 2015, Brown & et al., 2026, Chang & et al., 2022). These studies face several challenges, including lower image resolution, surface brightness dimming, limited photometric filter coverage, inconsistent rest-frame wavelengths, and uncertain stellar masses. In addition, limited photometry and a lack of galaxy spectroscopy can lead to inaccurate redshift estimates. This makes it more difficult to determine cluster membership and calculate accurate local galaxy densities (Brown & et al., 2026). Also, different methodologies for quantifying the environment yield different conclusions. For instance, some authors found the impact of the environment on their galaxy structures (Allen & et al., 2015, Brown & et al., 2026, Ding & et al., 2024), whereas some found no environmental effect on galaxies' structures (Abdullah, 2026, Figueira & et al., 2024).

Another important consideration is how to measure galaxy sizes. Most previous studies of the environmental dependence of galaxy structure have relied on sizes derived from galaxy light profiles. However, light-weighted sizes may not fully trace the underlying stellar mass distribution because galaxies can have

*rmand.mah@gmail.com, Corresponding author
†moein.mosleh@shirazu.ac.ir

doi: https://doi.org/10.52526/25792776-26.73.2-353

significant radial variations in their mass-to-light ratios (M_*/L). These variations are related to changes in stellar population age, metallicity, and dust content, and can produce color gradients across galaxies(Mosleh & et al., 2020, Suess & et al., 2019). As a result, two galaxies with similar light profiles may have different stellar mass distributions. Stellar mass profiles provide a more direct, robust description of how stellar mass is distributed within galaxies and are therefore better suited to studying the buildup of their central and outer regions. In particular, using mass-weighted sizes can reduce systematic effects caused by variations in color gradients and M_*/L between galaxies in different environments. Therefore, we use stellar mass-weighted sizes to investigate how galaxy structure depends on environment. To the best of our knowledge, this is the first study to use mass-weighted galaxy sizes to systematically investigate the role of environment in the galaxy mass–size relation. To further increase the sample size, we also extended our analysis to a larger set of galaxies using rest-frame NIR observations from JWST.

2. Data

To investigate how the environment affects the mass-size relation of galaxies, we use an environmental catalog derived by (Fossati & et al., 2017). They made publicly available a catalog of calibrated environmental measures for galaxies in the five 3D-HST/CANDELS (Skelton & et al., 2014) deep fields. They use the number density of neighbouring galaxies within fixed cylindrical apertures to characterize the environment of galaxies brighter than $JH140 < 24$ mag in the redshift range $0.5 < z < 3.0$. For each galaxy, the projected surface density within an aperture of radius $r_{\rm ap}$ is defined as $\Sigma_{r_{\rm ap}} = w_{r_{\rm ap}}/(\pi r_{\rm ap}^2)$, where $w_{r_{\rm ap}}$ is the sum of the weights of neighbouring galaxies within $r_{\rm ap}$ and a rest-frame velocity interval of ± 1500 km, s^{-1}. To account for the redshift evolution of the mean galaxy density, they define the overdensity as

$$\delta_{r_{\rm ap}} = \frac{\Sigma_{r_{\rm ap}} - \Sigma_{\rm mean}(z)}{\Sigma_{\rm mean}(z)}, \tag{1}$$

where $\Sigma_{\rm mean}(z)$ is the mean surface density at the corresponding redshift. The environmental density is then expressed as the logarithmic density contrast,

$$\log(1 + \delta_{r_{\rm ap}}). \tag{2}$$

We first cross-matched this with the catalog of stellar-mass-based galaxy sizes from Mosleh & et al. (2020). They estimated stellar mass maps from Hubble Space Telescope observations using pixel-by-pixel spectral energy distribution fitting for about 5,500 galaxies with stellar masses above $\log(M_\star/M_\odot) \geq 9.8$ up to redshift 2.0, in which 3052 objects were common to both catalogs. In addition, we used a morphological catalog from the DAWN JWST Archive (DJA) (Aurélien Genin & et al., 2025), which contains structural measurements for more than 340,000 galaxies over $0 < z < 12$ based on deep JWST/NIRCam imaging. We used the measurements obtained from the F444W imaging data. As a near-infrared band, F444W better probes rest-frame optical emission at high redshift. It is less affected by dust attenuation and the contribution of young stellar populations. The JWST-based measurements therefore provide a more suitable view of galaxy structure and complement the HST-based analysis.

3. Environmental & Star-Formation Activity Classification

We classified galaxies as star-forming or quiescent using the rest-frame UVJ color-color diagram, following (Williams & et al., 2009). After cross-matching these catalogs, we obtained a final sample of 3052 galaxies (Based on a stellar mass-based structural catalog): 2,261 star-forming and 791 quiescent. To analyze each parameter's role in galaxy structure, we binned each parameter. Table 1 describes the sub-samples we considered in detail.

We then extended our investigation to the JWST data-based catalog and redshift range of $0.5 < z < 3.0$. Again, we cross-matched the environmental catalog with the DJA morphological catalog and obtained a sample of about 12,000 objects, which we separated into star-forming and quiescent galaxies. Table 2 details the second sample.

Table 1. Summary of the environmental, redshift, and stellar-mass subsamples.

Property	**Sub-sample**	**Selection / Range**	N
Environment	Low density	$\log(1+\delta_{0.75}) < 0.2$	1624
	Mid density	$0.2 \leq \log(1+\delta_{0.75}) \leq 0.8$	1246
	High density	$\log(1+\delta_{0.75}) > 0.8$	182
Redshift	Low z	$0.5 \leq z < 1$	1444
	Mid z	$1 \leq z \leq 1.3$	982
	High z	$1.3 < z \leq 2$	626
Stellar Mass	Low mass	$9.8 \leq \log(M_*/M_\odot) \leq 10.4$	1836
	Mid mass	$10.4 < \log(M_*/M_\odot) \leq 10.8$	836
	High mass	$\log(M_*/M_\odot) > 10.8$	380

Table 2. Number and fraction of quiescent and star-forming galaxies in each redshift bin.

z**-bin**	**Total**	**Quiescent (Q)**	**Star-Forming (SF)**
$0.5-1.0$	4743	645 (13.6%)	4098 (86.4%)
$1.0-1.5$	3227	342 (10.6%)	2885 (89.4%)
$1.5-2.0$	2364	235 (9.9%)	2129 (90.1%)
$2.0-2.5$	1197	108 (9.0%)	1089 (91.0%)
$2.5-3.0$	282	16 (5.7%)	266 (94.3%)
Total	**11,813**	**1346 (11.4%)**	**10,467 (88.6%)**

4. Results

In the first step, we plotted the stellar-mass surface density profiles of star-forming and quiescent galaxies for the high-mass bin across three redshift bins. As shown in Fig. 1, environmental differences are very low for high-mass galaxies, and for both star-forming and quiescent galaxies across different redshifts, suggesting that massive systems are less sensitive to their local environment. Furthermore, at high redshifts, our sample in dense environments is extremely rare, which naturally limits our statistical analysis in that regime.

Fig. 2 shows the stellar mass-size relation across different redshift bins for both star-forming and quiescent populations. In bins where we have robust statistics—meaning a high number of galaxies—we observe no significant environmental dependence in the mass-size relation. In contrast, in bins with low galaxy counts, we see increased fluctuations. These variations likely reflect small-number statistics rather than any underlying physical environmental effect.

Fig. 3 shows the stellar mass–size relation for star-forming and quiescent galaxies in three redshift bins based on JWST data. The vertical dashed lines indicate the corresponding stellar mass completeness limits, above which the samples are considered complete and reliable. For star-forming galaxies (top row), galaxy size increases systematically with stellar mass across all three redshift bins. The relations for the low-, intermediate-, and high-density environments largely overlap, indicating no clear dependence of galaxy size on the local environment. Quiescent galaxies (bottom row) are substantially more compact than star-forming galaxies at comparable stellar masses. The most massive quiescent galaxies are predominantly found at redshifts below $z \sim 2.0$. Similar to the star-forming population, the mass–size relations of quiescent galaxies show no clear systematic dependence on the local environment.

5. Conclusion

While the environment is expected to play an important role in galaxy evolution, our results indicate that it has only a relatively weak impact on the galaxy stellar mass–size relation over the redshift range studied. For both star-forming and quiescent galaxies, we find no significant and systematic dependence of galaxy size on the local environment in either the HST- or JWST-based samples.

Instead, the galaxy mass–size relation strongly depends on stellar mass and redshift, with galaxy size increasing with stellar mass and evolving over cosmic time. The consistency between the HST and JWST results further suggests that the lack of a significant environmental dependence is robust against differences

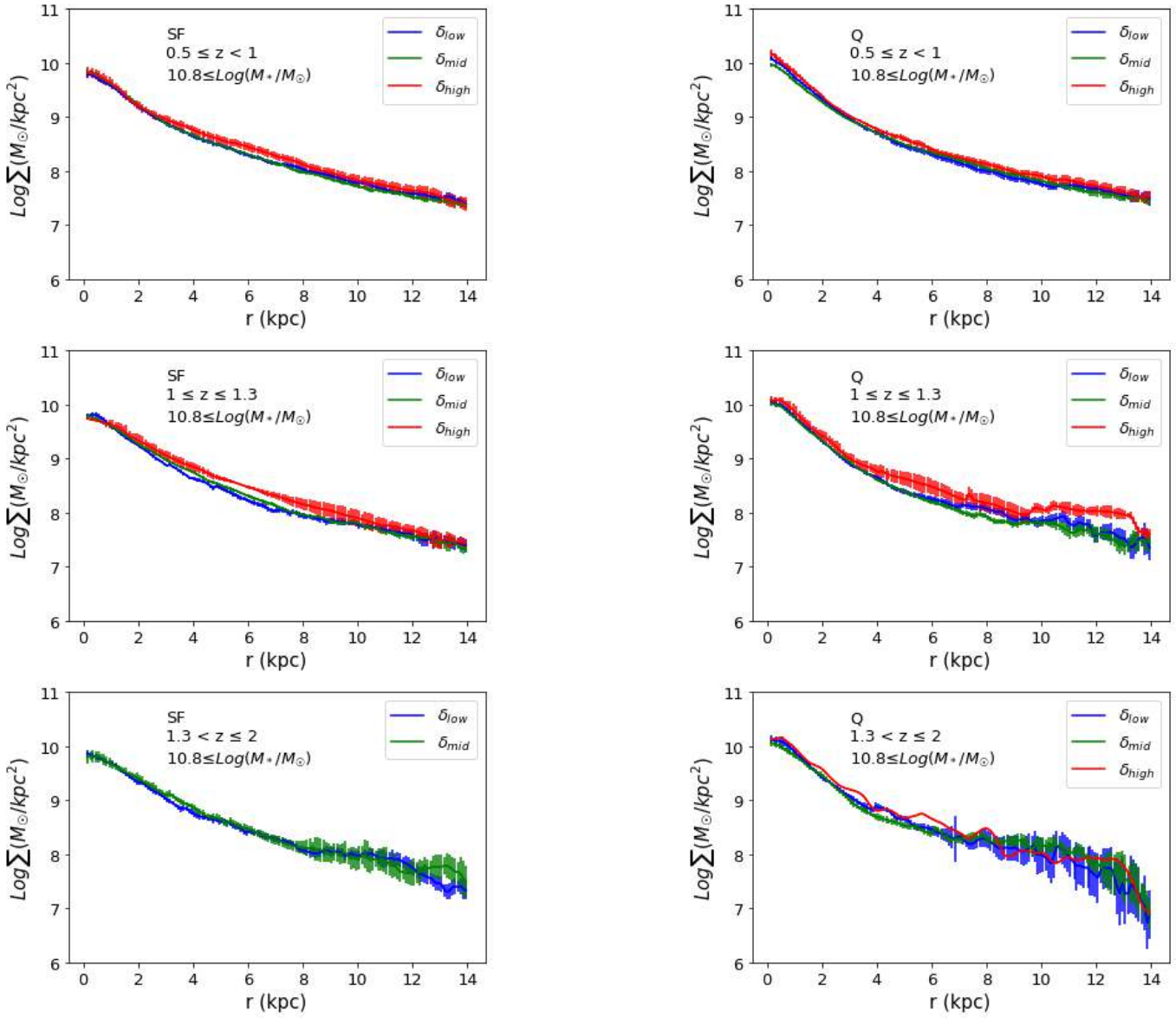

Figure 1. Stellar Mass Surface Density Profiles of Star-Forming and Quiescent Galaxies in redshift bins across different environments.

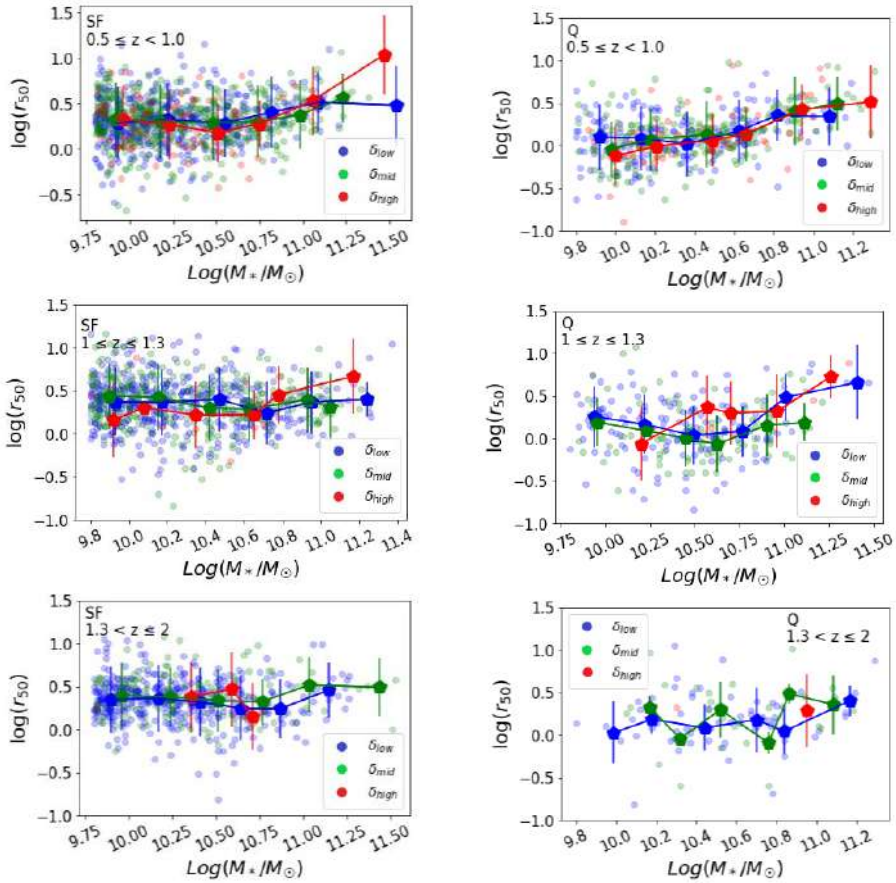

Figure 2. Stellar mass-size relation of star-forming and quiescent galaxies in different redshift bins using HST data. The relations for the low-, intermediate-, and high-density environments, shown in blue, green, and red.

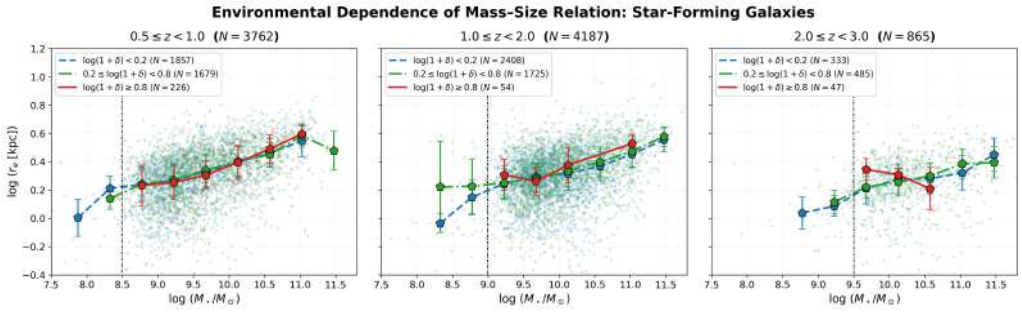

(a) Star-Forming Galaxies ($0.5 \leq z \leq 3.0$)

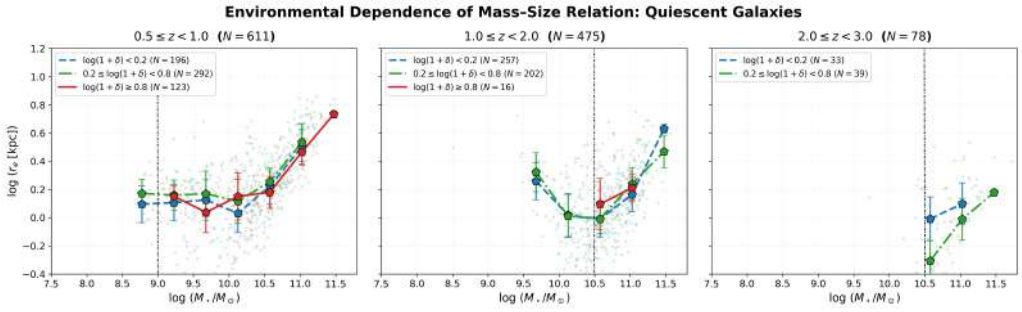

(b) Quiescent Galaxies ($0.5 \leq z \leq 3.0$)

Figure 3. Stellar mass–size relations for star-forming and quiescent galaxies in three redshift bins using JWST data. The relations for low-, intermediate-, and high-density environments are shown in blue, green, and red, respectively. The vertical dashed lines indicate the corresponding stellar mass completeness limits.

in sample size, wavelength, and structural measurement techniques, consistent with (Chang & et al., 2022, Figueira & et al., 2024)

doi: https://doi.org/10.52526/25792776-26.73.2-353

Overall, our results suggest that internal processes, rather than the local environment, dominate galaxy size evolution over $0.5 < z < 3.0$.

Future studies will extend this analysis to larger and better-constrained galaxy samples, combining more reliable redshift and environmental measurements with the growing availability of high-resolution JWST imaging. This will allow us to investigate environmental effects not only on the stellar mass–size relation, but also on other structural and physical properties of galaxies, including morphology, star formation activity, and quiescence. Exploring these properties simultaneously as functions of stellar mass, redshift, and environment will provide a more comprehensive picture of the relative roles of internal and environmental processes in galaxy evolution.

References

Abdullah Mohamed H. ; Abdelhamid N. E. . S. R. M. . W. G., 2026, The Astrophysical Journal, 1002, 173

Allen Rebecca J. ; Kacprzak G. G. . S. L. R., et al. 2015, The Astrophysical Journal, 806, 3

Aurélien Genin Marko Shuntov G. B., et al. 2025, Astronomy & Astrophysics, 699, A343

Brown Westley ; Muzzin A. . M. J. . W. G. ., et al. 2026, The Astrophysical Journal, 1007, 31

Chang Wenjun ; Fang G. . G. Y. . L. Z. ., et al. 2022, The Astrophysical Journal, 936, 47

Ding Y.; Zhu L. P. A., et al. 2024, Astronomy & Astrophysics, 686, A184

Figueira M. ; Siudek M. . P. A., et al. 2024, Astronomy & Astrophysics, 678, A117

Fossati M. ; Wilman D. J. . M. J. T., et al. 2017, The Astrophysical Journal, 835, 153

Mosleh Moein ; Hosseinnejad S. . H.-S. S. Z., et al. 2020, The Astrophysical Journal, 905, 170

Skelton Rosalind E. ; Whitaker K. E. . M. I. G., et al. 2014, The Astrophysical Journal Supplement Series, 214, 24

Suess Katherine A. ; Kriek M. . P. S. H., et al. 2019, The Astrophysical Journal, 877, 103

Williams R. J. Q. R. F. F. M. v. D. P., et al. 2009, The Astrophysical Journal, 691, 1